



# Investigation of Transport Properties of Some Superconductor Nickel-Based Antiperovskite $XNi_3$ ( $X = Mg, Al, Cu, Zn, Ga, Ag, Cd, In, Sn, Sb, Pt$ and $Pb$ )

Y. Benmalem<sup>1</sup> · A. Abbad<sup>1</sup> · W. Benstaali<sup>1</sup> · H. A. Bentounes<sup>2</sup> · T. Seddik<sup>3</sup> · T. Lantri<sup>1</sup>

Received: 4 January 2018 / Accepted: 12 March 2018 / Published online: 21 March 2018  
© Springer Science+Business Media, LLC, part of Springer Nature 2018

## Abstract

We report, in this work, a theoretical study of electronic and transport (thermoelectric) properties of some superconductor nickel-based antiperovskite  $XNi_3$  ( $X = Mg, Al, Cu, Zn, Ga, Ag, Cd, In, Sn, Sb, Pt$  and  $Pb$ ) using first-principles calculations with the full-potential linearized augmented plane wave (FP-LAPW) method based on the density functional theory (DFT) as implemented in the WIEN2k package. Electronic properties are calculated and show that the studied materials are of metallic type which is in good agreement with experimental data. The Seebeck coefficient, thermal conductivity, electrical conductivity and figure of merit were reported. The results obtained show that the zinc (Zn) and silver (Ag) materials are characterized by a high value of the figure of merit at room temperature (300 K) which is respectively 0.86 and 1.02 in a p-type region. In the case of the transition metals, the maximum values of  $S$  increase in going from the Pt atom to the Zn atom and then decrease for the Cd atom. Furthermore, the Wiedemann–Franz law which states that the ratio of thermal to electrical conductivity for metals is constant is well verified in this work. The electric conductivity values are almost invariant with the temperature except for the case of  $MgNi_3$  and  $AgNi_3$  compounds in which it increases with  $T$  slightly. So, the superconducting materials based on silver and zinc are the best for the thermoelectric applications at room temperature due to the very important value of the factor of merit and the Seebeck coefficient obtained.

**Keywords** Antiperovskites · Figure of merit · Seebeck coefficient · Thermal conductivity · Electric conductivity

## 1 Introduction

The study of the properties of thermoelectric (transport properties) materials is of great importance for many practical applications. This material turns heat into electricity more efficiently than anything available today. The theory of the generation of thermoelectric energy and thermoelectric refrigeration was presented for the first time by Altenkirch

in 1990 [1]. With the increasing world population and decreasing of conventional energy sources, the demand for electrical energy is growing rapidly [2]. Thermoelectric devices are reliable converters of energy, since they do not have moving mechanical parts and any noise or vibration [3]. Thermoelectricity is based on the principle of the direct conversion of heat to electricity [4], and its efficiency depends on the operating temperatures, the figure of merit and the design configuration including the external load parameter of the device [5].

In thermoelectric (TE) appliances, a sufficient amount of heat can be converted into an amount of useful energy [6]. The dimensionless figure of merit,  $ZT = \sigma S^2 T / k$ , is a key material parameter, linked to the efficiency, where  $\sigma$  is the electrical conductivity,  $S$  is the Seebeck coefficient and  $k$  is the thermal conductivity, composed of electronics and lattice parts [7]. The materials with  $ZT$  above the unit are considered to be excellent candidates for TE applications [8, 9]. A variety of research groups

✉ W. Benstaali  
ben\_wissam@yahoo.fr

<sup>1</sup> Laboratory of Technology and Solids Properties, Abdelhamid Ibn Badis University, 27000 Mostaganem, Algeria

<sup>2</sup> Abdelhamid Ibn Badis University, 27000 Mostaganem, Algeria

<sup>3</sup> Laboratoire de Physique Quantique et de Modélisation Mathématique, Université de Mascara, 29000 Mascara, Algeria

have synthesized thermoelectric properties of different crystal structures such as skutterudites [10], clathrates [11], full-Heusler alloys [12], chalcogenides [13], oxide complex [14, 15] and perovskites [16, 17]. Many of physical properties of the antiperovskite structure compounds were studied after the discovery of the first antiperovskite superconductor MgCNi<sub>3</sub> in 2001 [18, 19]. The appearance of superconductivity pushed researchers to study Ni-based antiperovskite, especially elastic properties, but no thermoelectric properties were reported before. For this reason, we have taken a series of antiperovskite materials in the form of XNNi<sub>3</sub> (where X = Mg, Al, Cu, Zn, Ga, Ag, Cd, In, Sn, Sb, Pt and Pb) to determine the suitable materials for thermoelectric applications. The objective of this study is to predict theoretically and to give a broad understanding of the transport properties of these antiperovskites, since it has not been initiated either by other theories or other experimental tests.

## 2 Calculation

All the calculations of antiperovskite compounds were performed via the full-potential linearized augmented plane wave (FP-LAPW) method [16–20], which is known to be a precise and efficient approach to solve the Kohn–Sham equation within a framework of the DFT as implemented in the WIEN2k code [21, 22]. The generalized gradient approximation (GGA) proposed by Wu–Cohen (WC-GGA) [23] was used for exchanges and correlation. The values of lattice constants of these materials are taken from ref [24]. The separation energy between the core and valence states is kept at  $-7.0$  Ry. The wave functions inside the atomic spheres in the fullpotential scheme for these materials are expanded in terms of spherical harmonics up to  $l_{\max} = 10$ .

The convergence parameter  $RMT \times K_{\max}$  is set to 7. One thousand  $k$ -points are used for electronic property calculations. The RMTs used for these materials are presented in Table 1. The compounds have a cubic crystal structure with a space group of Pm-3m (no. 221). In the unit cell, the first atoms (X = Mg, Al, Cu, Zn, Ga, Ag, Cd, In, Sn, Sb, Pt and Pb) are found in the corners (0, 0, 0), the second atom (N) is located at the body center (0.5, 0.5, 0.5) and the three atoms (Ni) are located at (0.5, 0, 0), (0, 0.5, 0) and (0; 0; 0.5) positions.

To ensure the convergence of the transport properties, we need a large number of  $k$ -points for the thermoelectric properties of all the compounds and we used 100000  $k$ -points in the irreducible wedge of the Brillouin zone (IWBZ). In this work, the thermoelectric properties such as the Seebeck coefficients, the thermal conductivities and the electrical conductivities are calculated using the BoltzTraP

**Table 1** RMT values for each element of MgNNi<sub>3</sub>, AlNNi<sub>3</sub>, CuNNi<sub>3</sub>, ZnNNi<sub>3</sub>, GaNNi<sub>3</sub>, AgNNi<sub>3</sub>, CdNNi<sub>3</sub>, InNNi<sub>3</sub>, SnNNi<sub>3</sub>, SbNNi<sub>3</sub>, PtNNi<sub>3</sub> and PbNNi<sub>3</sub>

Compound	Elements	RMT
MgNNi <sub>3</sub>	Mg	1.8
	N	1.5
	Ni	2.0
AlNNi <sub>3</sub>	Al	1.8
	N	1.5
	Ni	2.0
CuNNi <sub>3</sub>	Cu	2.0
	N	1.5
	Ni	1.8
ZnNNi <sub>3</sub>	Zn	2.0
	N	1.5
	Ni	1.8
GaNNi <sub>3</sub>	Ga	2.0
	N	1.5
	Ni	1.8
AgNNi <sub>3</sub>	Ag	2.5
	N	1.5
	Ni	1.8
CdNNi <sub>3</sub>	Cd	2.2
	N	1.5
	Ni	1.8
InNNi <sub>3</sub>	In	2.2
	N	1.5
	Ni	1.8
SnNNi <sub>3</sub>	Sn	2.2
	N	1.5
	Ni	1.8
SbNNi <sub>3</sub>	Sb	2.2
	N	1.5
	Ni	1.8
PtNNi <sub>3</sub>	Pt	2.5
	N	1.5
	Ni	1.8
PbNNi <sub>3</sub>	Pb	2.5
	N	1.5
	Ni	1.8

[25] code. Equation (1) interprets the transport coefficients, which are based on the rigid band approach to conductivity

$$\sigma_{\alpha\beta}(\varepsilon) = \frac{1}{N} \sum_{i,k} \sigma_{\alpha\beta}(i, k) \frac{\delta(\varepsilon - \varepsilon_{i,k})}{\delta(\varepsilon)} \quad (1)$$

$$\sigma_{\alpha\beta}(i, \vec{k}) = e^2 \tau_{i,k} \mathbf{v}_{\alpha}(i, \vec{k}) \mathbf{v}_{\beta}(i, \vec{k}) \quad (2)$$

where  $N$  is the number of  $k$ -points. Equation (2) explains  $K$ -dependent transport tensors, where  $\tau$  is the relaxation time

and  $\mathbf{v}_\alpha(i, \vec{k})$  is the component of group speeds. Depending on the temperature ( $T$ ) and the chemical potential ( $\mu$ ) the transport coefficients as the electrical conductivity, Seebeck coefficient tensors and electronic thermal conductivity can be found by integrating the transport distribution [25, 26]

$$\sigma_{\alpha\beta}(T, \mu) = \frac{1}{\Omega} \int \sigma_{\alpha\beta}(\varepsilon) \left[ -\frac{\partial \mathbf{f}_0(T, \varepsilon, \mu)}{\partial \varepsilon} \right] d\varepsilon \quad (3)$$

$$S_{\alpha\beta}(T, \mu) = \frac{1}{eT\Omega\sigma_{\alpha\beta}(T, \mu)} \int \sigma_{\alpha\beta}(\varepsilon) (\varepsilon - \mu) \left[ -\frac{\partial \mathbf{f}_0(T, \varepsilon, \mu)}{\partial \varepsilon} \right] d\varepsilon \quad (4)$$

$$k_{\alpha\beta}^0(T, \mu) = \frac{1}{e^2 T \Omega} \int \sigma_{\alpha\beta}(\varepsilon) (\varepsilon - \mu)^2 \left[ -\frac{\partial \mathbf{f}_0(T, \varepsilon, \mu)}{\partial \varepsilon} \right] d\varepsilon \quad (5)$$

where  $\alpha$  and  $\beta$  are the tensor indices,  $e$  is the electron charge,  $\Omega$  is the volume of the unit cell,  $\mu$  is the carrier concentration and  $\mathbf{f}$  is the Fermi–Dirac distribution function. The relaxation time ( $\tau$ ) is kept constant in this study. The Seebeck coefficient is calculated by the band structure calculation because it does not depend on the relaxation time (under the assumption that relaxation time is constant) but the electrical conductivity must be calculated relative to the relaxation time.

### 3 Results and Discussion

#### 3.1 Electronic Properties

We used the GGA to generate better predictions of the band structure. The band structure diagrams for  $X\text{NNi}_3$  ( $X = \text{Mg, Al, Cu, Zn, Ga, Ag, Cd, In, Sn, Sb, Pt}$  and  $\text{Pb}$ ) are shown in Fig. 1. We can see clearly that these antiperovskite materials have a metallic character because of the overlap of the valence bands with the conduction bands and the Fermi level passes through the overlapping regions. We also note from Fig. 2 that the orbitals of the conduction band exceed the Fermi level to be in the valence band as in the case of materials ( $\text{PtNNi}_3, \text{SnNNi}_3, \text{CuNNi}_3$  and  $\text{SbNNi}_3$ ) which confirms that the studied materials are of metallic type.

To powerfully understand the electronic properties of the antiperovskites studied, we have computed the total density of states using GGA, and to explain the contribution of different states in the band structures, partial densities of states are also calculated and shown in Figs. 3, 4 and 5. For all the compounds studied, one can notice easily strong hybridization between  $\text{Ni-}3d$  and  $\text{N-}2p$  states around the Fermi level which comes to confirm the metallicity of all the materials, except for  $\text{PbNNi}_3$  and  $\text{SnNNi}_3$  where we can

see, in addition, a contribution from  $\text{Pb/Sn-}5s$  states and, for  $\text{PtNNi}_3$ , some  $\text{Pt-}5d$  states. For  $\text{PbNNi}_3$  and  $\text{PtNNi}_3$ , the contribution of  $4f$  states is not shown here since it is very low. In addition, we can see clearly that for some compounds such as  $\text{CuNNi}_3, \text{PbNNi}_3$  and  $\text{PtNNi}_3$ , Fermi energy cuts a narrow band, and for others such as  $\text{AlNNi}_3, \text{GaNNi}_3$  and  $\text{ZnNNi}_3$ , Fermi energy cuts a narrow band. All these differences will affect the transport properties as we can see later, and the findings will change from a compound to another.

#### 3.2 Thermoelectric Properties

The electricity generation in electric thermoelectric generators is based on direct physical conversions of heat into electricity. This physical phenomenon motivated the researchers to find several conventional sources of energy and to search materials characterized by low thermal conductivity as in the glass, and high electrical conductivity as in crystals [27, 28]. The efficiency of thermoelectric devices is determined by the figure of merit ( $ZT$ ), and this coefficient includes the three parameters which describe the thermoelectric materials: Seebeck coefficient ( $S$ ), electric conductivity ( $\sigma / \tau$ ) and thermal conductivity ( $k / \tau$ ).

##### 3.2.1 Seebeck Coefficient

The appearance of a potential difference at the junction of two materials subjected to a temperature difference represents the Seebeck effect. The Seebeck coefficient is defined as the open circuit voltage produced between two points on a conductor, where a uniform temperature difference of 1 K exists between these points. The Seebeck coefficient varies with the level of the temperature at which the temperature difference occurs. For a good thermoelectric device, we need a high Seebeck coefficient. Figures 6 and 7 show the variation of Seebeck coefficient for nickel-based superconducting materials at 300, 600 and 900 K according to the chemical potential. From the analysis of all figures, it is clear that for all title materials, the maximum value of Seebeck coefficient is reached in the p-type region with the highest value achieved by the  $\text{ZnNNi}_3$  compound which is of about  $472 \mu\text{V/K}$  at room temperature. In addition, the low maximum values of Seebeck coefficient in the p-type region is  $30 \mu\text{V/K}$ , which correspond to the  $\text{PtNNi}_3$  compound. Consequently, it is evident that the best thermoelectric response can be realized in the p-type region. However, one can remark that some compounds such as  $\text{AgNNi}_3$  and  $\text{ZnNNi}_3$  present good values of  $S$  in the n-type region, and this highlighted that this two compounds could also be a good n-type thermoelectric when suitably doped with electrons. Since the DOS around the Fermi level plays an important role for transport properties, the

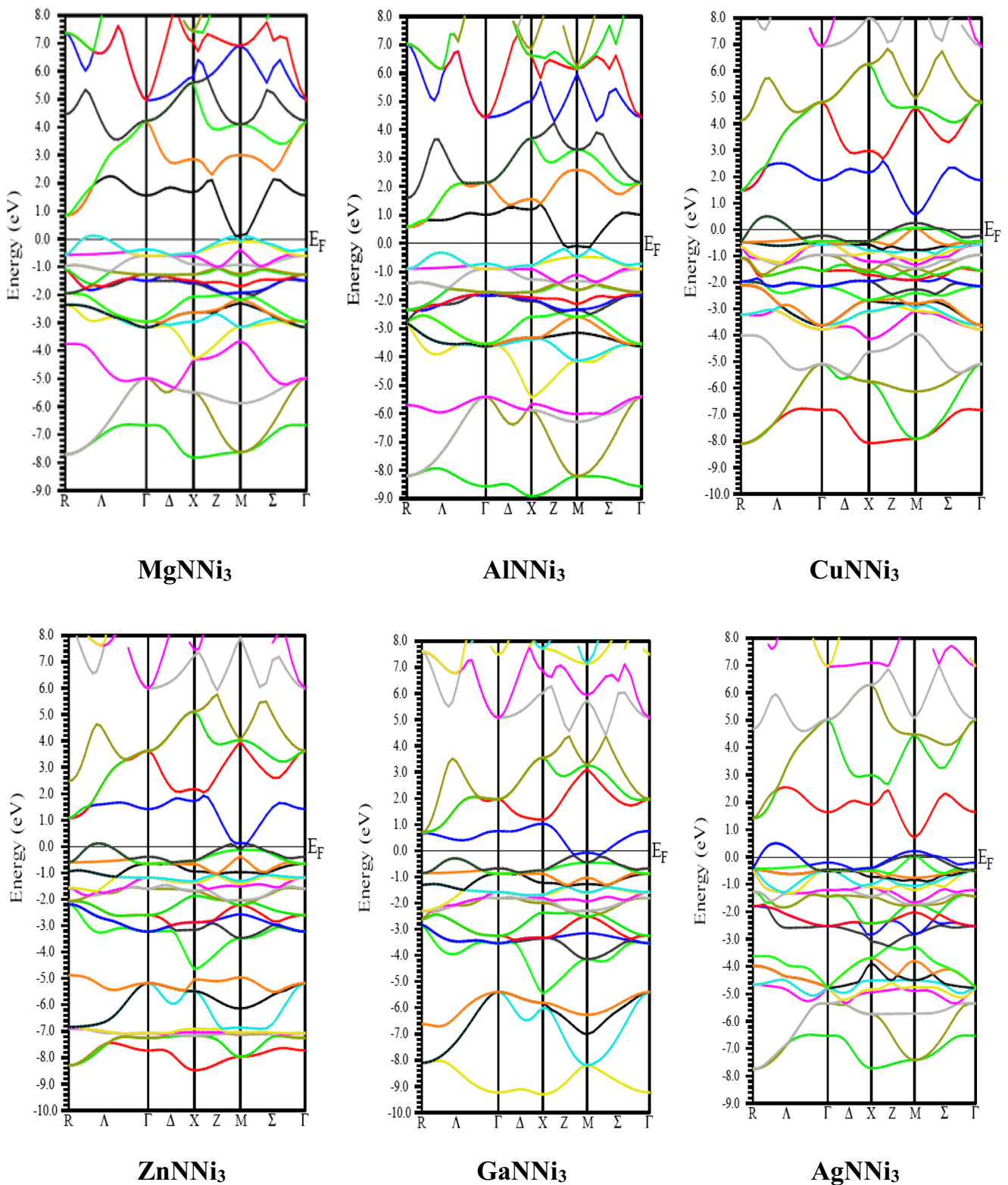


**Fig. 1** Calculated band structures of MgNNi<sub>3</sub>, AlNNi<sub>3</sub>, CuNNi<sub>3</sub>, ZnNNi<sub>3</sub>, GaNNi<sub>3</sub> and AgNNi<sub>3</sub>

Ni-3*d* and N-2*p* states are responsible for the thermoelectric effects. Thus, the presence of the Pt-5*d* states in the Fermi level has directly affected the transport properties

of PtNNi<sub>3</sub> compound which show low maximum values of Seebeck coefficient in the p-type region. On the other hand, the absence of all the states of Zn atom around



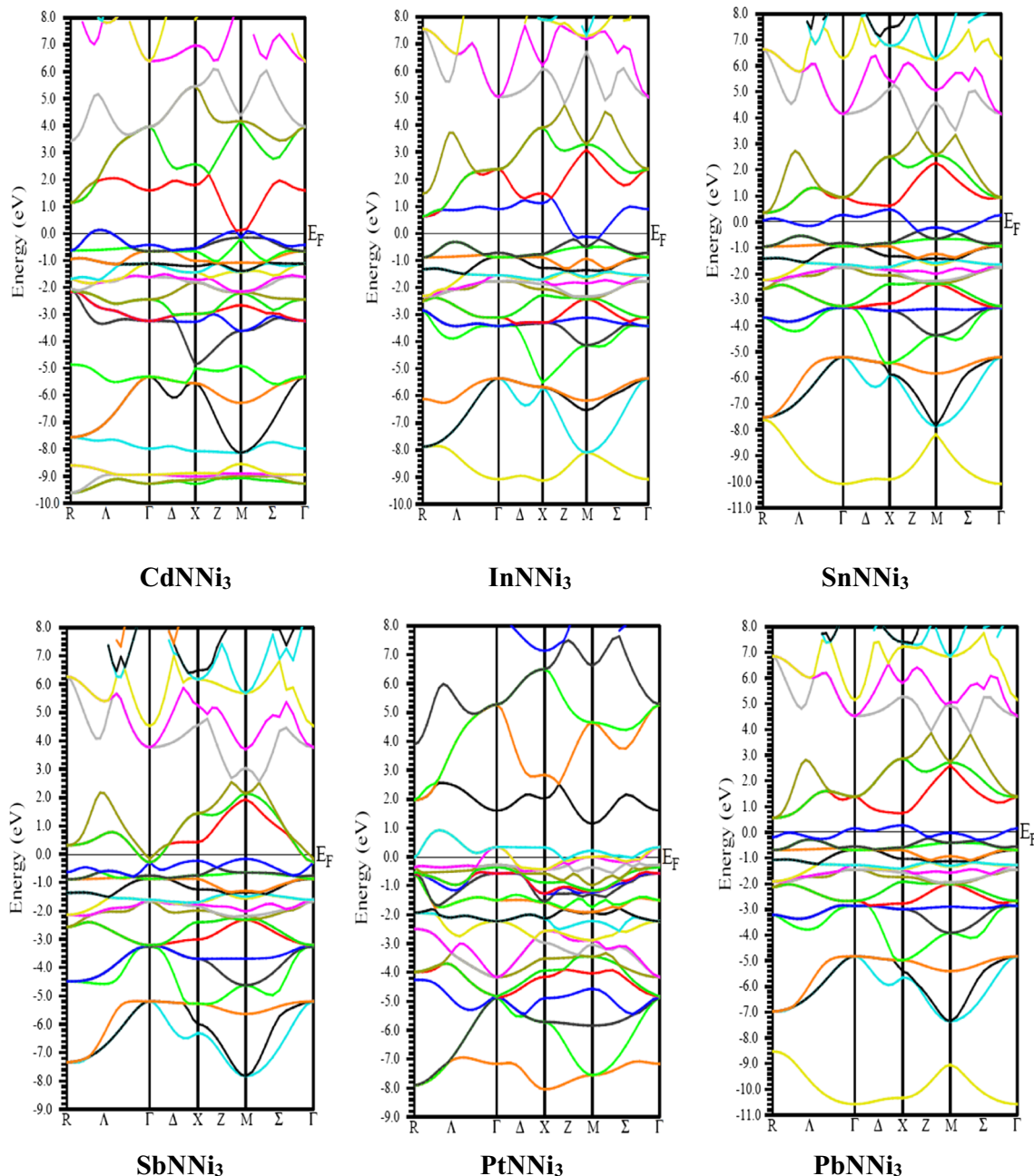


**Fig. 2** Calculated band structures of CdNNi<sub>3</sub>, InNNi<sub>3</sub>, SnNNi<sub>3</sub>, SbNNi<sub>3</sub>, PtNNi<sub>3</sub> and PbNNi<sub>3</sub>

the Fermi level make the ZnNNi<sub>3</sub> compound show the highest thermoelectric power. Furthermore, in the case of the transition metals, the maximum values of  $S$  increase in going from the Pt atom to the Zn atom and then decrease for the Cd atom. Conversely, there is a maximum decrease in magnitude as one moves downward within period III, i.e. from Al to In, which is the same case from the Sn atom to the Pb atom. This trend mainly comes from the shift of the Fermi level upward, deeper in the conduction band (see Figs. 6 and 7). At room temperature, Table 2 gives the Seebeck coefficient of all the materials studied in this paper.

### 3.2.2 Electric Conductivity

The electric conductivity depends on the mobility of carriers that is influenced by the impurities and defects. The electrons move in a material from the hot region to the cold one, and the current is produced as a result of this phenomenon. For a good thermoelectric device, the materials must have a high electrical conductivity [29].

Figures 8 and 9 show the electric conductivity of the series of antiperovskites discussed in this paper at 300, 600 and 900 K according to the chemical potential. The

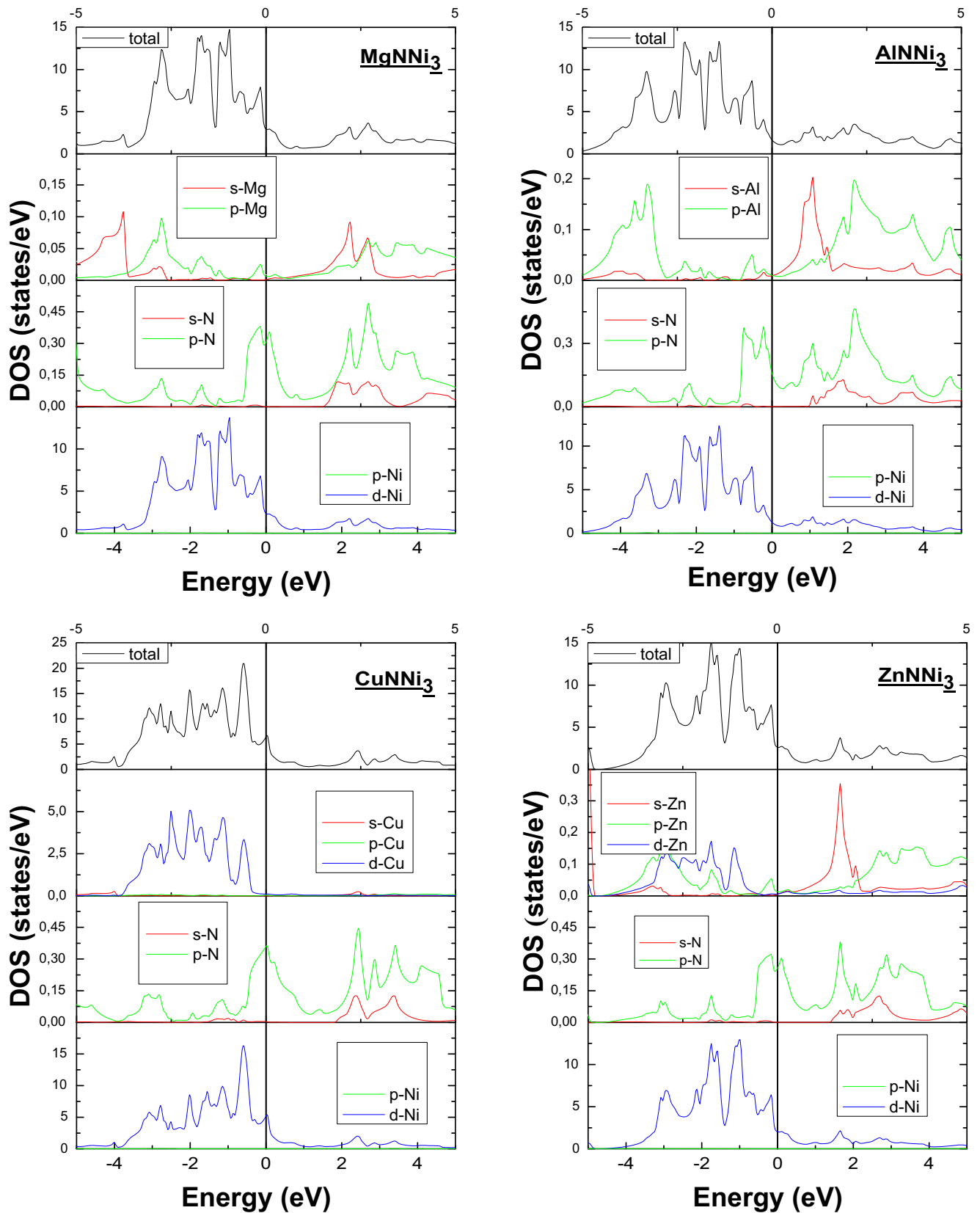


Fig. 3 Total and partial density of states of MgNNi<sub>3</sub>, AlNNi<sub>3</sub>, CuNNi<sub>3</sub> and ZnNNi<sub>3</sub>

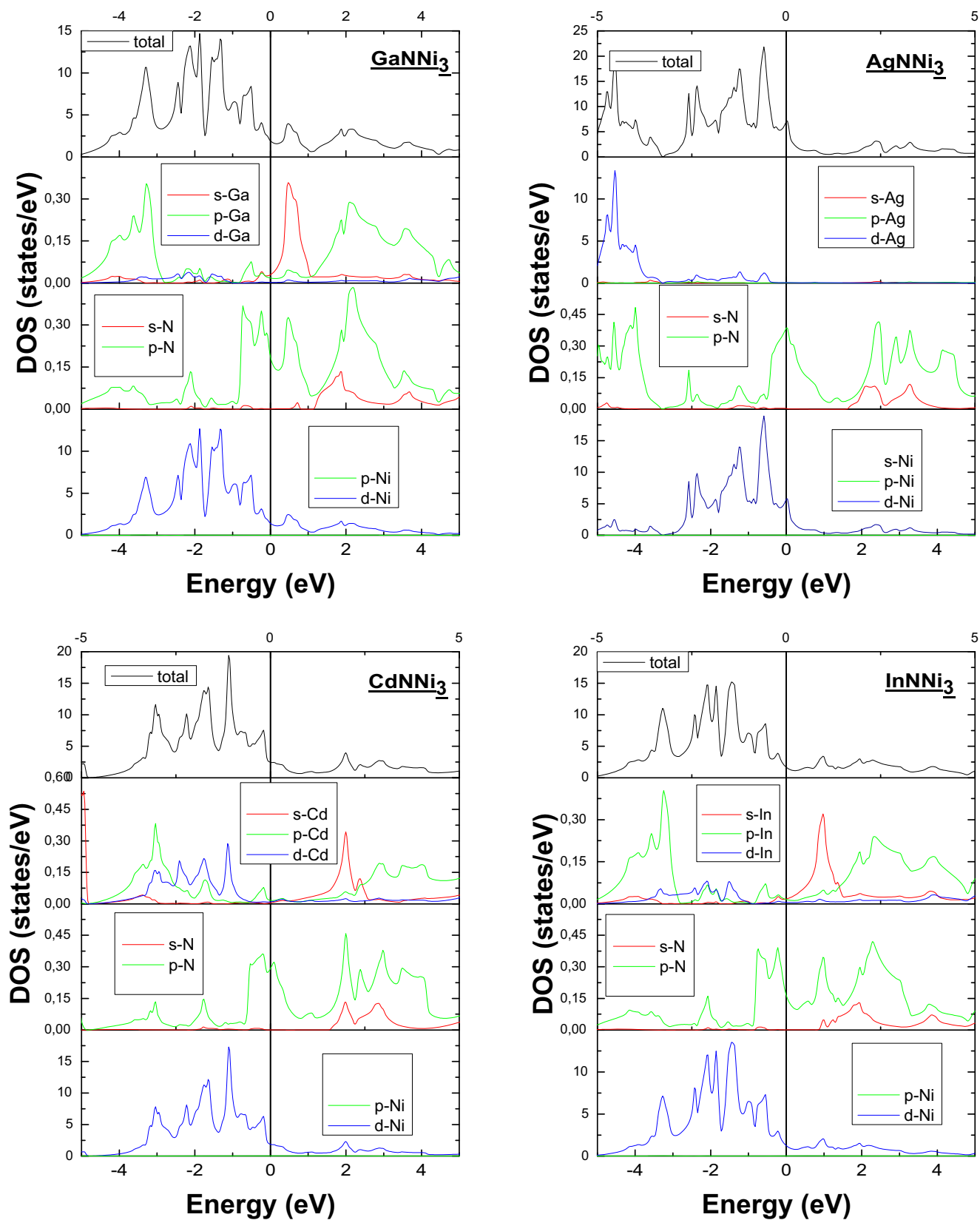


Fig. 4 Total and partial density of states of GaNNi<sub>3</sub>, AgNNi<sub>3</sub>, CdNNi<sub>3</sub> and InNNi<sub>3</sub>

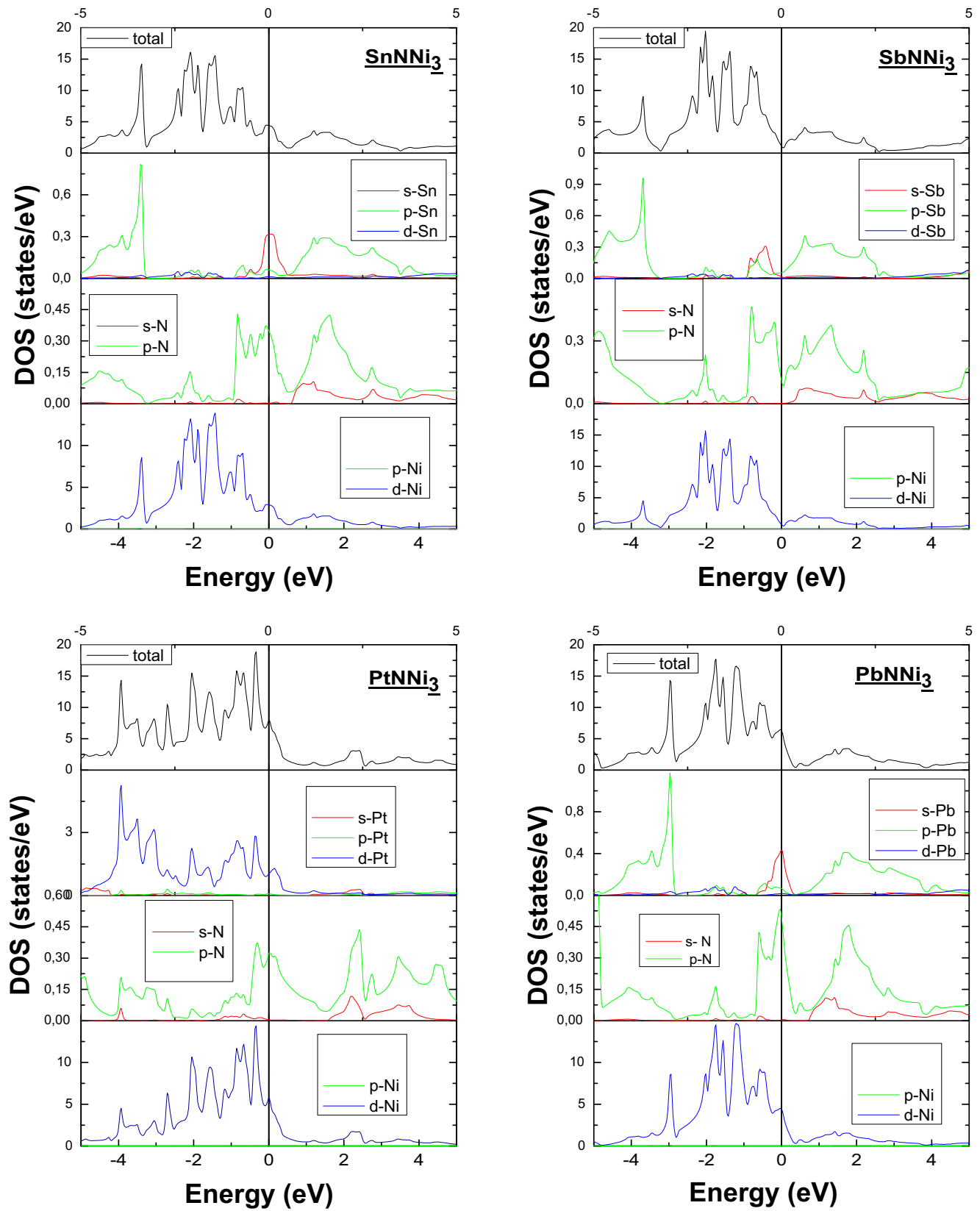
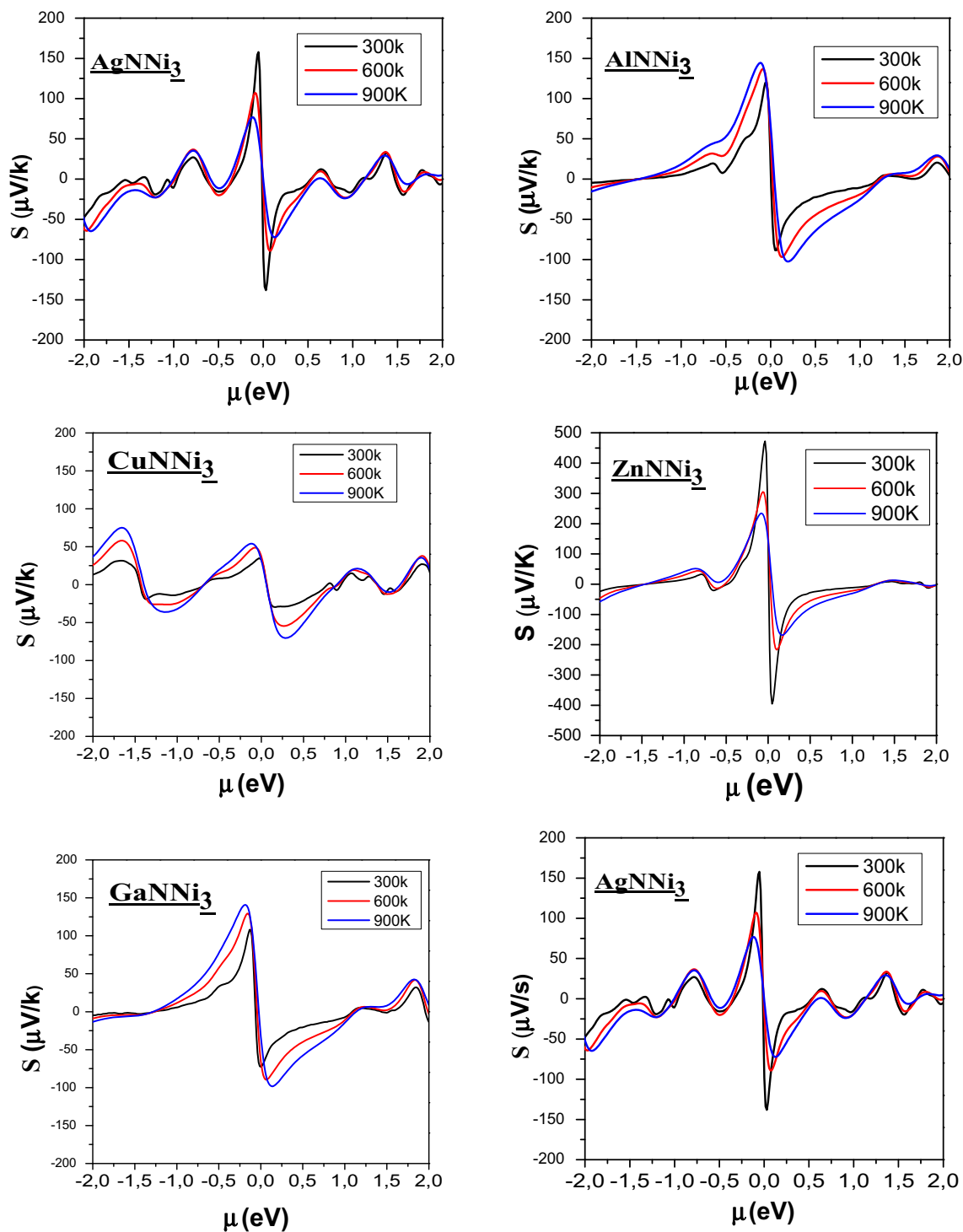


Fig. 5 Total and partial density of states of  $\text{SnNNi}_3$ ,  $\text{SbNNi}_3$ ,  $\text{PtNNi}_3$  and  $\text{PbNNi}_3$



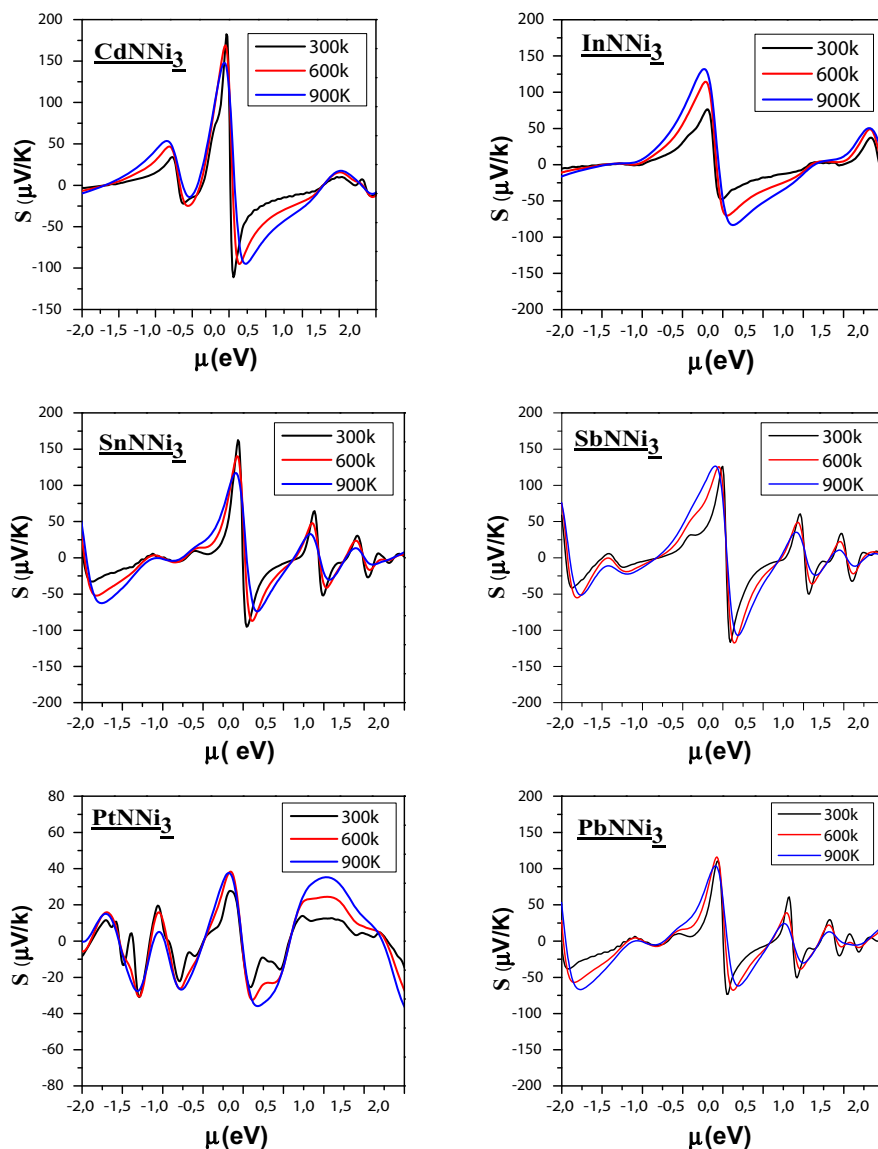


**Fig. 6** Seebeck coefficient of  $\text{MgNNi}_3$ ,  $\text{AlNNi}_3$ ,  $\text{CuNNi}_3$ ,  $\text{ZnNNi}_3$ ,  $\text{GaNNi}_3$  and  $\text{AgNNi}_3$  as a function of chemical potential at 300, 600 and 900 K

figures show clearly that the electrical conductivity for all materials is minimal between  $-0.25\mu$  (eV) and  $0.25\mu$  (eV); beyond this range, the electric conductivity increases with increasing chemical potential. The behavior of all

materials with respect to temperature is almost similar, and the curves for the three temperatures (300, 600 and 900 K) are getting closer. We notice here that according to the approximate expressions of the electrical conductivity,  $\sigma$  is

**Fig. 7** Seebeck coefficient of PtNNi<sub>3</sub>, CdNNi<sub>3</sub>, InNNi<sub>3</sub>, SnNNi<sub>3</sub>, SbNNi<sub>3</sub>, PtNNi<sub>3</sub> and PbNNi<sub>3</sub> as a function of chemical potential at 300, 600 and 900 K



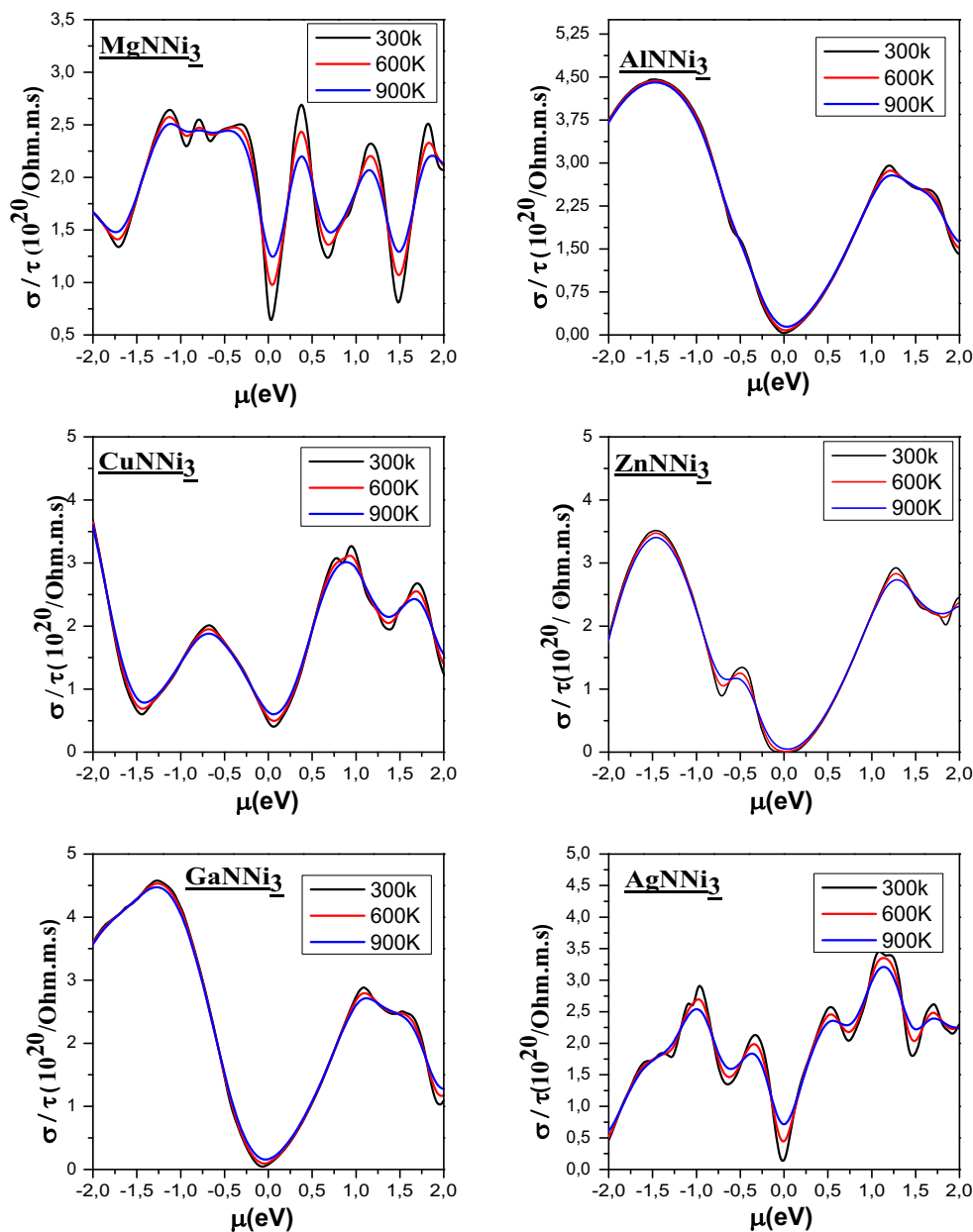
not concerned with  $T$  but depends on the DOS (or transport distribution function). So, as our investigated materials are metallic, when  $T$  increases, the Fermi levels are still within the conduction bands and the DOSs in the Fermi windows ( $\partial f / \partial \varepsilon$ ) do not change significantly. Therefore, the  $\sigma$  values are almost invariant except for the case of MgNNi<sub>3</sub> and AgNNi<sub>3</sub> compounds in which the  $\sigma$  increases with  $T$  slightly at  $\mu = 0$ .

We can also observe that the maximum value of electric conductivity at room temperature is obtained for the PtNNi<sub>3</sub> material which ranges up to  $5.6 \times 10^{20} / \Omega \text{ms}$  at  $0.5 \mu$  (eV) chemical potential. For the rest of the antiperovskites studied, the maximum value of the electric conductivity reached at room temperature is  $3.45 \times 10^{20} / \Omega \text{ms}$  at  $1 \mu$  (eV) chemical potential for AgNNi<sub>3</sub>,  $2.95 \times 10^{20} / \Omega \text{ms}$  at  $1 \mu$  (eV) chemical potential for AlNNi<sub>3</sub>,  $4 \times 10^{20} / \Omega \text{ms}$  at  $-1.6 \mu$  (eV) chemical potential for CdNNi<sub>3</sub>,  $3.26 \times$

**Table 2** Seebeck coefficient in microvolts per Kelvin, thermal conductivity ( $k/\tau$ ) in  $10^{15}$  W/Kms, electric conductivity ( $\sigma/\tau$ ) in  $10^{20} / \Omega \text{ms}$ , figure of merit ( $ZT$ ) and Lorentz number ( $L$ ) in  $10^{-8}$  W/ $\Omega \text{K}^2$  at room temperature

Compound	$S$	$ZT$	$k/\tau$	$\sigma/\tau$	$L$
MgNNi <sub>3</sub>	70	0.17	1.86	2.67	2.32
AlNNi <sub>3</sub>	112	0.30	3.24	4.46	2.42
CuNNi <sub>3</sub>	34.5	0.04	2.42	3.57	2.25
ZnNNi <sub>3</sub>	472	0.85	2.54	3.55	2.37
GaNNi <sub>3</sub>	103	0.30	3.31	4.57	2.41
AgNNi <sub>3</sub>	157	1.02	2.16	3.17	2.27
CdNNi <sub>3</sub>	179	0.50	3.24	4.46	2.42
InNNi <sub>3</sub>	74	0.18	1.49	2.06	2.41
SnNNi <sub>3</sub>	159	0.50	1.75	2.62	2.22
SbNNi <sub>3</sub>	124	0.35	2.13	2.95	2.40
PtNNi <sub>3</sub>	25	0.02	2.26	3.46	2.17
PbNNi <sub>3</sub>	104	0.32	1.67	2.36	2.35

**Fig. 8** Electric conductivity of MgNNi<sub>3</sub>, AlNNi<sub>3</sub>, CuNNi<sub>3</sub>, ZnNNi<sub>3</sub>, GaNNi<sub>3</sub> and AgNNi<sub>3</sub> as a function of chemical potential at 300, 600 and 900 K

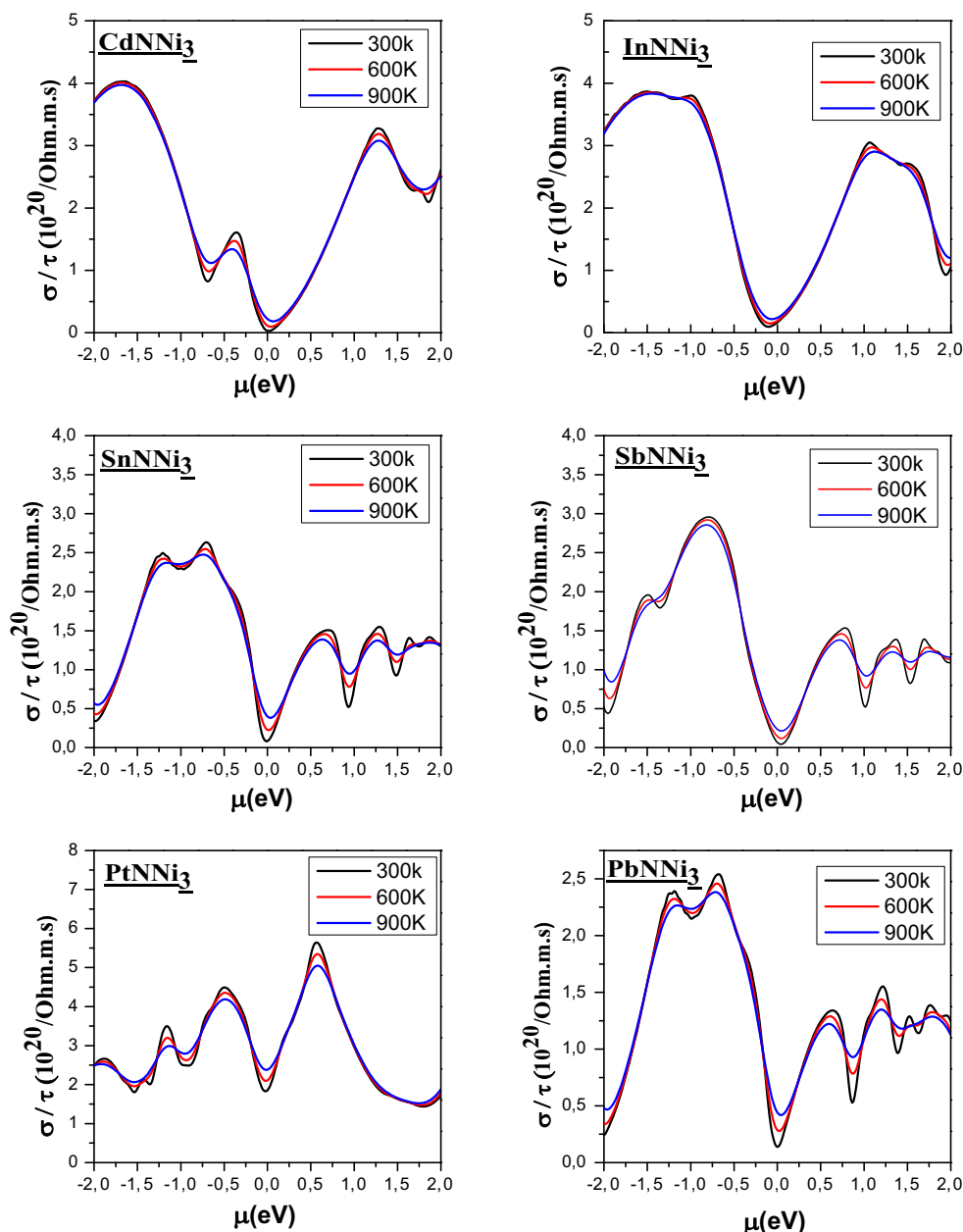


$10^{20}/\Omega\text{ms}$  at  $0.9\mu$  (eV) chemical potential for CuNNi<sub>3</sub>,  $4.57 \times 10^{20}/\Omega\text{ms}$  at  $-1.2\mu$  (eV) chemical potential for GaNNi<sub>3</sub>,  $3.86 \times 10^{20}/\Omega\text{ms}$  at  $-1.5\mu$  (eV) chemical potential for InNNi<sub>3</sub>,  $2.69 \times 10^{20}/\Omega\text{ms}$  at  $0.37\mu$  (eV) chemical potential for MgNNi<sub>3</sub>,  $2.54 \times 10^{20}/\Omega\text{ms}$  at  $-0.67\mu$  (eV) chemical potential for PbNNi<sub>3</sub>,  $2.95 \times 10^{20}/\Omega\text{ms}$  at  $-0.79\mu$  (eV) chemical potential for SbNNi<sub>3</sub>,  $2.63 \times 10^{20}/\Omega\text{ms}$  at  $-0.7\mu$  (eV) chemical potential for SnNNi<sub>3</sub>, and  $3.51 \times 10^{20}/\Omega\text{ms}$  at  $-1.46\mu$  (eV) chemical potential for ZnNNi<sub>3</sub>.

### 3.2.3 Thermal Conductivity

The optimization of thermoelectric materials also depends on an important factor called thermal conductivity which is the transfer of energy in the form of heat due to a difference in temperature within a material or between materials. Overall, the thermal conductivity ( $k = k_e + k_l$ ) comprises of the electronic contribution ( $k_e$ ) and the lattice contribution ( $k_l$ ), and this later is insignificant compared to  $k_e$  in

**Fig. 9** Electric conductivity of PtNi<sub>3</sub>, CdNi<sub>3</sub>, InNi<sub>3</sub>, SnNi<sub>3</sub>, SbNi<sub>3</sub>, PtNi<sub>3</sub> and PbNi<sub>3</sub> as a function of chemical potential at 300, 600 and 900 K

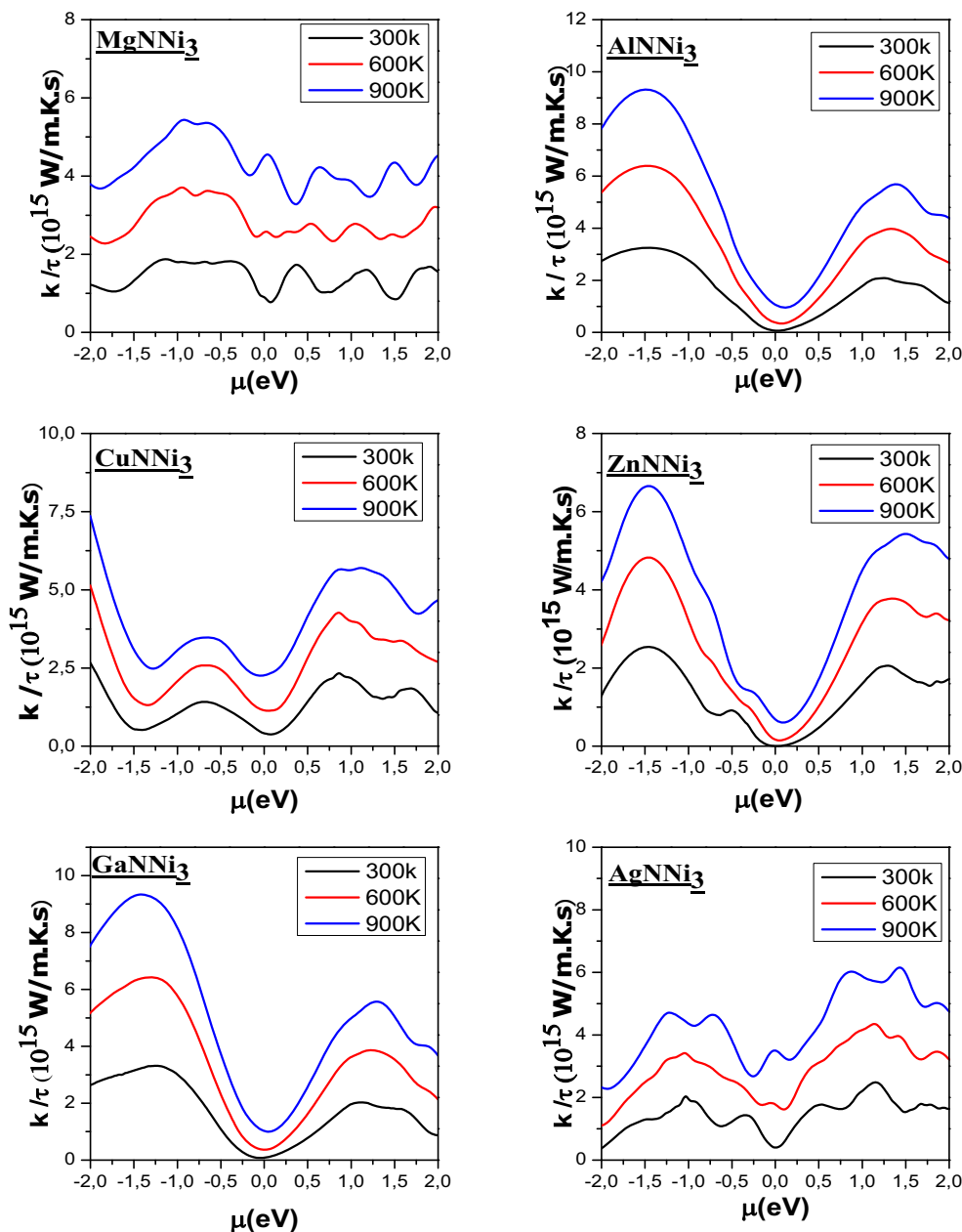


most metals. Besides, the electronic thermal conductivity ( $k_e$ ) is connected to the electronic conductivity via the Wiedemann–Franz law as follows:  $k_e = L\sigma T$ , where  $L$  is the Lorentz number and is equal to  $2.44 \times 10^{-8} \text{ J}^2/\text{K}^2/\text{C}^2$  for free electrons. So, a good thermoelectric material requires a low thermal conductivity, without degrading the electrical conductivity.

Figures 10 and 11 show the evolution of the thermal conductivity according to the chemical potential at 300, 600 and 900 K for all the superconducting materials discussed in this work. From the two figures, we can see that the

thermal conductivity of all nickel-based materials is almost zero between  $-0.25$  and  $0.25 \mu\text{V}$ . It is also observed that the thermal conductivity is proportional to the increase in temperature since following the Wiedemann–Franz law, the electrical conductivity is almost constant and thus the temperature increases are responsible for the enhancing of  $k_e$ . The results obtained in this work indicate a relatively high thermal conductivity value for any material having a fairly high electrical conductivity as shown by the case of the material presented (PtNi<sub>3</sub>) which represents the maximum value of the thermal conductivity; therefore, the

**Fig. 10** Thermal conductivity of MgNNi<sub>3</sub>, AlNNi<sub>3</sub>, CuNNi<sub>3</sub>, ZnNNi<sub>3</sub>, GaNNi<sub>3</sub> and AgNNi<sub>3</sub> as a function of chemical potential at 300, 600 and 900 K

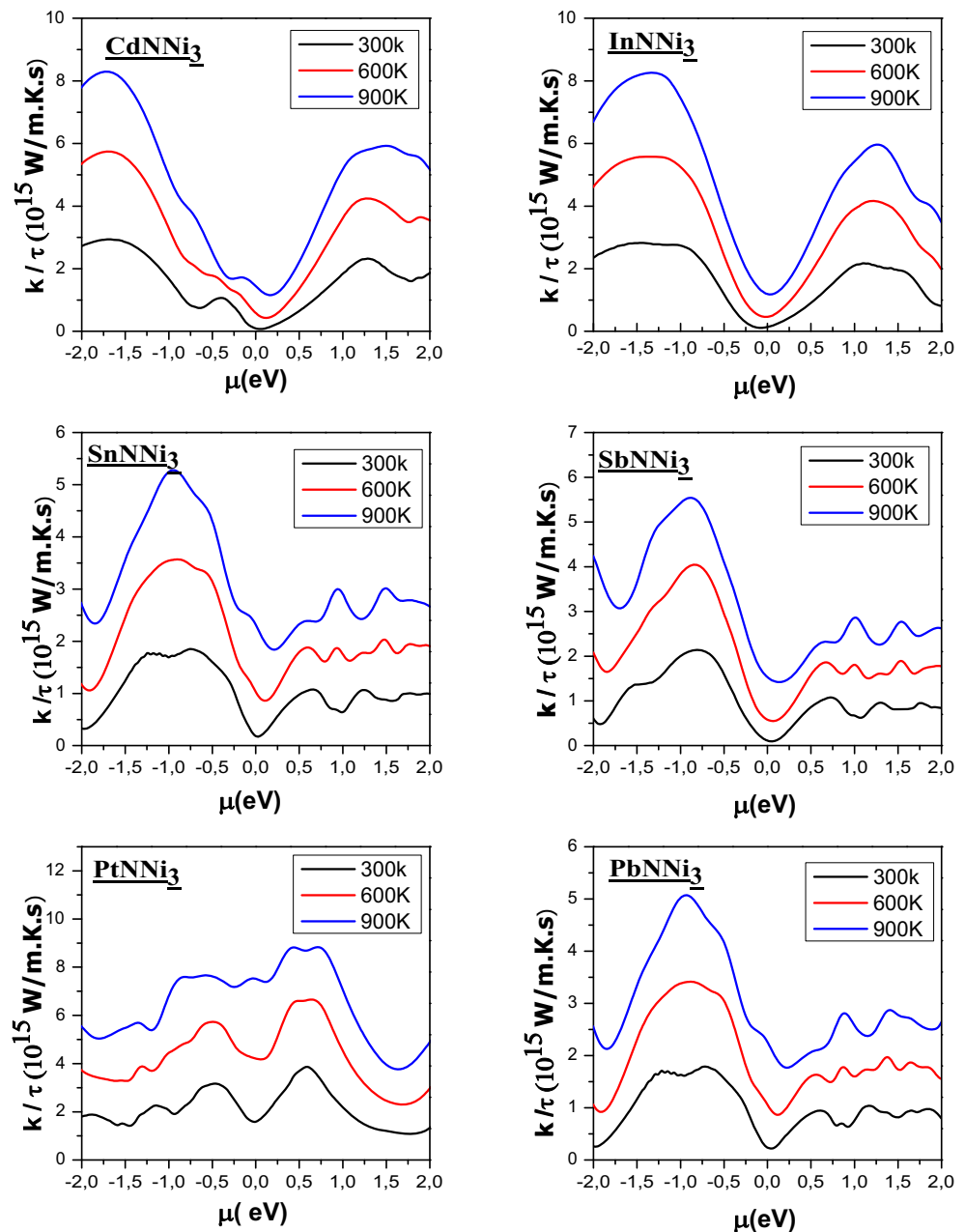


Wiedemann–Franz law is well verified in this work (see Table 2), and our findings confirm the efficiency of the law.

The thermal conductivity increases when one moves away from  $\mu = 0$ . The significance of this increase is related to the definition of the chemical potential that can be described as a force of attraction between the atoms that causes the lattice vibrations; so, an increase of this phenomenon of vibration increases the value of the thermal conductivity of the material. The ZnNNi<sub>3</sub> compound is a good thermal conductor compared to the other materials studied with the  $5 \times 10^{11} \text{ W/Kms}$  thermal conductivity at

room temperature and at  $0\mu$  (eV) chemical potential and with a maximum value of approximately  $25 \times 10^{14} \text{ W/Kms}$  at  $-1.5\mu$  (eV) chemical potential. Also for GaNNi<sub>3</sub> and AlNNi<sub>3</sub>, a low value of  $8 \times 10^{13} \text{ W/Kms}$  is depicted at  $0\mu$  (eV) chemical potential. For the rest of the antiperovskites studied, the minimum thermal conductivity is  $10^{14} \text{ W/Kms}$  for CdNNi<sub>3</sub>, InNNi<sub>3</sub> and SbNNi<sub>3</sub>,  $2 \times 10^{14} \text{ W/Kms}$  for PbNNi<sub>3</sub> and SnNNi<sub>3</sub>,  $4 \times 10^{14} \text{ W/Kms}$  for AgNNi<sub>3</sub> and  $8 \times 10^{14} \text{ W/Kms}$  for MgNNi<sub>3</sub>, and finally, the high value concerns PtNNi<sub>3</sub> which is about  $15 \times 10^{14} \text{ W/Kms}$  always at  $0\mu$  (eV) chemical potential.

**Fig. 11** Thermal conductivity of PtNNi<sub>3</sub>, CdNNi<sub>3</sub>, InNNi<sub>3</sub>, SnNNi<sub>3</sub>, SbNNi<sub>3</sub>, PtNNi<sub>3</sub> and PbNNi<sub>3</sub> as a function of chemical potential at 300, 600 and 900 K



### 3.2.4 Figure of Merit

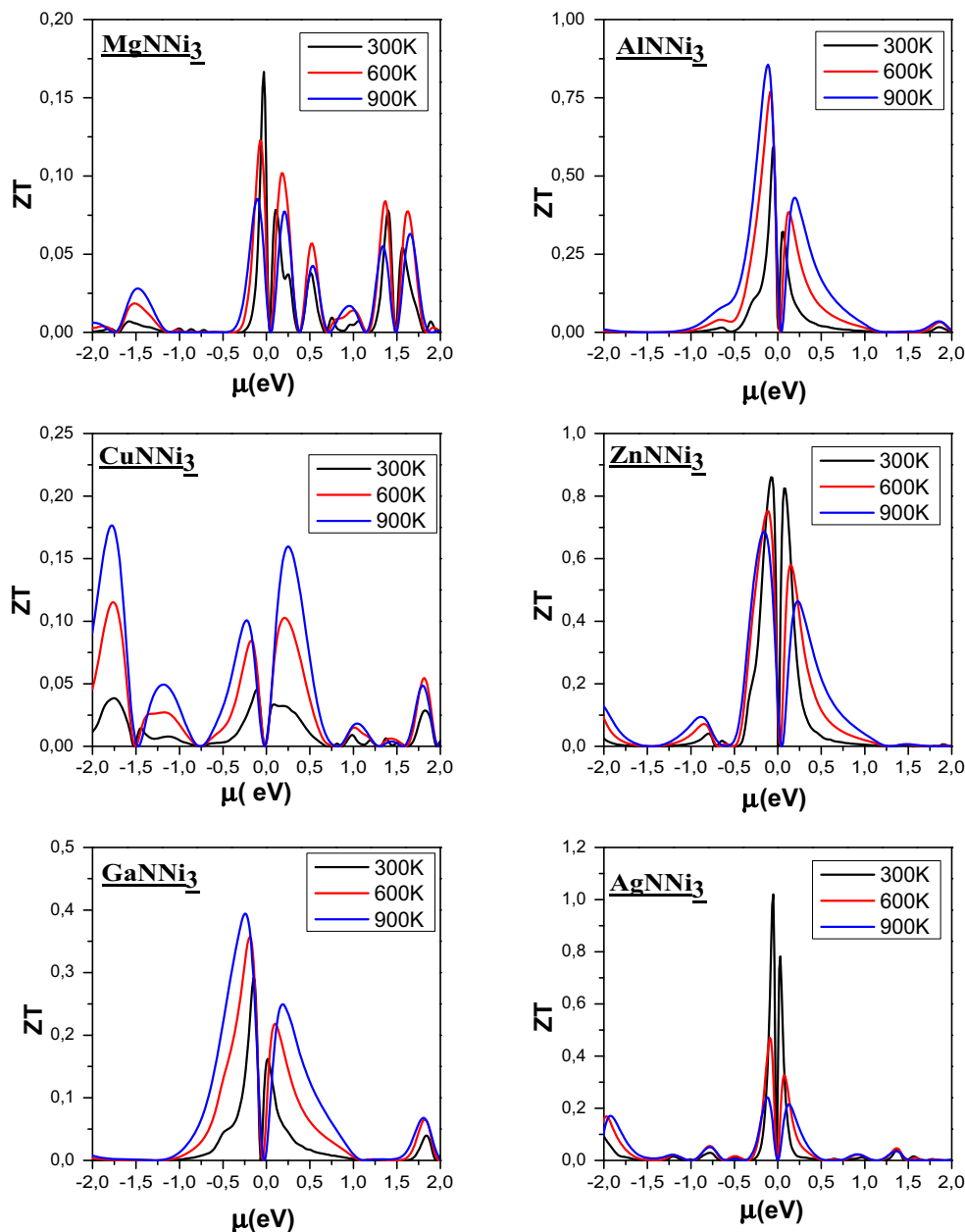
The figure of merit ( $ZT$ ) represents a dimensionless number that predicts the performances of a thermoelectric material. The figure of merit ( $ZT$ ) is mathematically described by the following relation:  $ZT = \sigma S^2 T / k$  [30], where  $T$  is the absolute temperature (in Kelvin),  $S$  the thermoelectric power (or coefficient of Seebeck),  $\sigma$  the electrical conductivity and  $K$  the thermal conductivity.

The coefficient of merit ( $ZT$ ) is greater for high coefficients of Seebeck ( $S$ ). It is proportional to the ratio of the electrical conductivity ( $\sigma$ ) to the thermal conductivity ( $K$ ).

The material defined by a  $ZT$  greater than or equal to the unit represents the best elements for the thermoelectric devices. Figures 12 and 13 represent the figure of merit according to the chemical potential at 300, 600 and 900 K of XNNi<sub>3</sub> (X = Mg, Al, Cu, Zn, Ga, Ag, Cd, In, Sn, Sb, Pt and



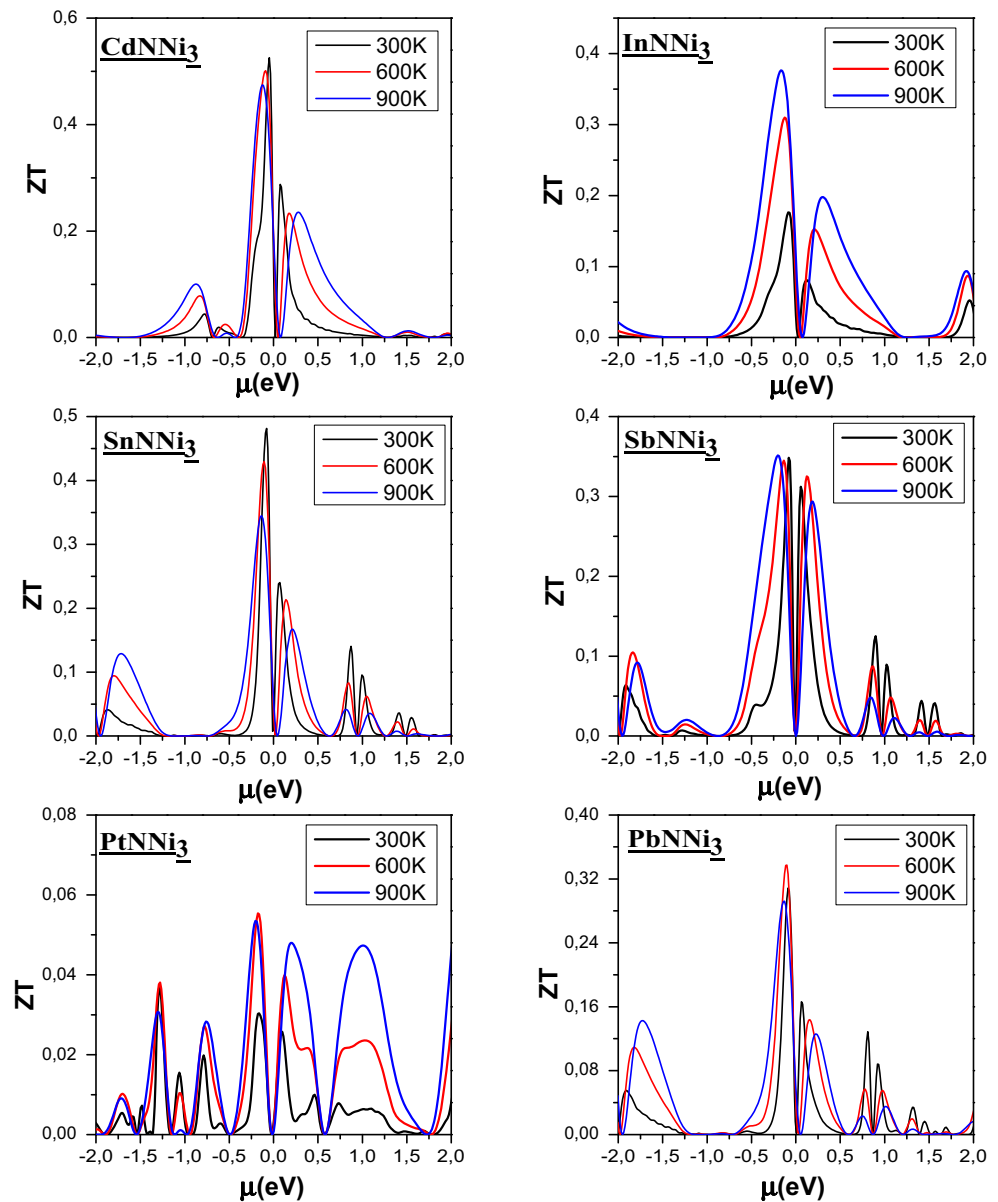
**Fig. 12** Figure of merit of  $\text{MgNNi}_3$ ,  $\text{AlNNi}_3$ ,  $\text{CuNNi}_3$ ,  $\text{ZnNNi}_3$ ,  $\text{GaNNi}_3$  and  $\text{AgNNi}_3$  as a function of chemical potential at 300, 600 and 900 K



Pb). From these figures, we can notice that both materials ( $\text{AgNNi}_3$  and  $\text{ZnNNi}_3$ ) are characterized by high figures of merit of about 1.02 and 0.86 in the p-type region and of about 0.78 and 0.82 in the n-type region, respectively. The figures show also that the value of the figure of merit starts to decrease beyond zero until reaching  $-0.25\mu$  (eV) and  $0.25\mu$  (eV), so this region is the area of the good response of the material where a high Seebeck coefficient and a low thermal conductivity are depicted, the reason why we have

a good factor of merit factor. The zinc and silver materials have almost the same behavior in both n- and p-type regions. For the rest of the nickel-based antiperovskites, the values of the figure of merit found in this work at room temperature are as follows: 0.59, 0.52, 0.04, 0.29, 0.34, 0.17, 0.16, 0.30, 0.03 and 0.48 for  $\text{AlNNi}_3$ ,  $\text{CdNNi}_3$ ,  $\text{CuNNi}_3$ ,  $\text{GaNNi}_3$ ,  $\text{SbNNi}_3$ ,  $\text{InNNi}_3$ ,  $\text{MgNNi}_3$ ,  $\text{PbNNi}_3$ ,  $\text{PtNNi}_3$  and  $\text{SnNNi}_3$ , respectively. We should precise that, for some antiperovskites such as  $\text{AlNNi}_3$ ,  $\text{CuNNi}_3$ ,  $\text{GaNNi}_3$

**Fig. 13** Figure of merit of PtNNi<sub>3</sub>, CdNNi<sub>3</sub>, InNNi<sub>3</sub>, SnNNi<sub>3</sub>, SbNNi<sub>3</sub>, PtNNi<sub>3</sub> and PbNNi<sub>3</sub> as a function of chemical potential at 300, 600 and 900 K



and InNNi<sub>3</sub>, ZT is maximal at 900 K so these materials can be good thermoelectric candidates at high temperature.

#### 4 Conclusion

The use of the BoltzTraP code based on the FPLAPW method allowed us to study a series of nickel-based antiperovskite metallic materials, where we obtained results on their electronic and, for the first time, thermoelectric properties. Since the density of states around the Fermi level plays an important role for transport properties, electronic properties are calculated and show that the studied materials are of metallic type which is in good agreement with experimental reports and the Ni-3*d* and

N-2*p* states are responsible for the thermoelectric effects. For thermoelectric properties, a good behavior of the materials was noted at room temperature, so we found a very strong Seebeck coefficient for the ZnNNi<sub>3</sub> material which is equal to 472 μV/K at 0μ (eV) and even a high electric conductivity with a low thermal conductivity and that between  $-0.25\mu$  (eV) and  $0.25\mu$  (eV) of chemical potential. These parameters resulted in a high merit factor in an order of 1.02 and 0.86 in the p-type region and of about 0.78 and 0.82 in the n-type region for silver- and zinc-based materials, respectively. Also, the Wiedemann–Franz law which states that the ratio of thermal to electrical conductivity for metals is constant is well verified in this work.

Nickel-based superconducting materials can be proposed for thermoelectric applications and considered as a source

of low-temperature energy to produce electricity. PtNNi<sub>3</sub> antiperovskite has a high electrical conductivity but, in the same time, a high thermal conductivity and a very low figure of merit. Also, GaNNi<sub>3</sub> and AlNNi<sub>3</sub> have a low thermal conductivity but a medium figure of merit; as a result, our aim from this study is to give wide information about all the thermoelectric parameters of this series of antiperovskites and the researchers choose the suitable element for it. We specify that our results are open to experimental verifications.

## References

1. Xi, H., Luo, L., Fraisse, G.: *Renew. Sustain. Energy Rev.* **11**(5), 923 (2007)
2. Budak, S., Alim, M.A., Bhattacharjee, S., Muntele, C.: *Phys. Procedia* **66**, 321 (2015)
3. Riffat, S.B., Xiaoli, M.: *Appl. Therm. Eng.* **23**, 913 (2003)
4. Budak, S., Guner, S., Minamisawa, R.A., Muntele, C.I., Ila, D.: *Appl. Surf. Sci.* **310**, 226 (2014)
5. Sahin, A.Z., Yilbas, B.S.: *Energ. Conver. Manage.* **65**, 26 (2013)
6. Bell, L.E.: *Science* **321**, 1457 (2008)
7. Qu, X., Wang, W., Liu, W., Yang, Z., Duan, X., Jia, D.: *Mater J. Chem. Phys.* **129**, 331 (2011)
8. Rabina, O., Lin, Y.M., Dresselhaus, M.S.: *Appl. Phys. Lett.* **79**, 81 (2001)
9. Takeuchi, T.: *Mater. Trans.* **50**, 2359 (2009)
10. Aliabad, H.A.R., Ghazanfari, M., Ahmad, I., Saeed, M.A.: *Comput. Mater. Sci.* **65**, 509 (2012)
11. Blake, N.P., Latturmer, S., Bryan, J.D., Stucky, G.D., Metiu, H.: *J. Chem. Phys.* **115**, 8060 (2001)
12. Gupta, D.C., Ghosh, S.: *J. Supercond. Novel Magn.*, 1 (2017)
13. Harman, T.C., Taylor, P.J., Walsh, M.P., LaForge, B.E.: *Science* **297**, 2229 (2002)
14. Matsubara, I., Funahashi, R., Takeuchi, T., Sodeoka, S.: *Appl. Phys. Lett.* **90**, 462 (2001)
15. Shin, W., Murayama, N., Ikeda, K., Sago, S.: *J. Power Sources* **103**, 80 (2001)
16. Terasaki, I., Sasago, Y., Uchinokura, K.: *Phys. Rev. B* **56**, 12685 (1997)
17. Maignan, A., Wang, L.B., Hebert, S., Pelloquin, D., Raveau, B.: *Chem. Mater.* **14**, 1231 (2002)
18. He, T., Huang, Q., Ramirez, A.P., Wang, Y., Regan, K.A., Rogado, N., Hayward, M.A., Haas, M.K., Slusky, J.S., Inumara, K., Zandbergen, H.W., Ong, N.P., Cava, R.J.: *Nature* **411**, 54 (2001)
19. Bilal, M., Ahmad, I., Rahnamaye-Aliabad, H.A., Jalali-Asadabadi, S.: *Comput. Mater. Sci.* **85**, 310 (2014)
20. Engel, E., Vosko, S.H.: *Phys. Rev. B* **47**, 13164 (1993)
21. Andersen, O.K.: *Phys. Rev. B* **12**, 3060 (1975)
22. Kohn, W., Sham, L.: *Phys. Rev. B* **140**, A1133 (1965)
23. Hohenberg, P., Kohn, W.: *Phys. Rev.* **136**, B864 (1964)
24. Bannikov, V.V., Shein, I.R., Ivanovskii, A.L.: *Physica B* **405**, 4615 (2010)
25. Madsen, G.K.H., Singh, D.J.: *Comput. Phys. Commun.* **175**, 67 (2006)
26. Scheidemantel, T.J., Ambrosch-Draxl, C., Thonhauser, T., Badding, J.V., Sofo, J.O.: *Phys. Rev. B* **68**, 125210 (2003)
27. Noda, Y., Kon, H., Furukawa, Y., Otsuka, N., Nishida, I.A., Masumoto, K.: *Materials transactions. JIM* **33**, 845 (1992)
28. Slack, G.A.: *Thermoelectric handbook*. Edition. Rowe DM. Chemical Rubber company. Boca Raton, 407 (1995)
29. Rabin, O., Yu-Ming, L., Dresselhaus, M.S.: *Appl. Phys. Lett.* **79**, 81 (2001)
30. Walia, S., Weber, R., Balendhran, S., Yao, D., Abrahamson, J.T., Zhuiykov, S., Bhaskaran, M., Sriram, S., Strano, M.S., Kalantar-zadeh, K.: *Chem. Commun.* **48**, 7462 (2012)